Title

Sedimentary Basin Site Response for Different Basin Types in Southern California

Authors

Nweke, Chukwuebuka C
Stewart, Jonathan
Wang, Pengfei
et al.

Publication Date

2022-07-01

Peer reviewed

12th National Conference on Earthquake Engineering
Salt Lake City, Utah
27 June - 1 July 2022
Hosted by the Earthquake Engineering Research Institute

Sedimentary Basin Site Response for Different Basin Types in Southern California

C. C. Nweke,[1] J. P. Stewart,[2] P. Wang,[3] and S. J. Brandenberg[4]

ABSTRACT

Site response effects are described by ergodic ground motion models, which are developed using global data from sites with diverse site conditions, using the time-averaged shear-wave velocity in the upper 30 m (V_{S30}) and isosurface depths ($z_{1.0}$ or $z_{2.5}$). Site responses in sedimentary basins may have specific dependencies on the geometry and extent of the sedimentary structure in addition to V_{S30} and isosurface depths. We investigate here the effects of basin-to-basin categorization on site response. Using southern California data, we highlight differences in mean site amplification for eight large sedimentary basins with different geologic origins. The mean response in all basins shows significant relative amplification at long periods (T > 0.5 sec) and none at shorter periods (T < 0.3 sec). Comparisons of basin-specific responses reveal that coastal basins exhibit greater levels of relative long-period amplification than inland, fault-bounded sedimentary basins.

Introduction

Sedimentary basins are formed from a variety of geologic processes that include subsidence (sinking ground), spreading zones (rifts), and faults (dropping blocks, pulling-apart, wrenching) [1]. These forming mechanisms induce variations in dimensions (lateral and vertical extents), shape, and orientation, leading to complex features that vary between basins [2]. Moreover, the depositional environment under which the accumulation of sediments occurred also introduces significant variability to the evolution of a basin. From an engineering perspective, basins are depressions on the earth's surface filled with sedimentary deposits that are deep and decrease in thickness towards their margins [3]. Examples of basins include the Valley of Mexico basin (including Mexico City) [4], the Kathmandu basin in Nepal [5], and the Los Angeles basin in California [6].

In the NGA-West2 ground motion models (GMM), basin seismic responses are represented using a combination of a shallow profile indicator via the time-averaged shear-wave velocity in the upper 30 m (V_{S30}), and a deep profile indicator via the depth to a 1 km/s or 2.5 km/s shear-wave velocity isosurface horizon ($z_{1.0}$ or $z_{2.5}$). In addition to basin sites, there are also small-scale sediments, colluvial deposits, and weathered zones in mountainous/hilly areas. Because similar values of V_{S30} and isosurface depth may occur both in basins and other sedimentary structures, ergodic models are unable to differentiate between site responses in basins and non-basins. Nweke et al. 2022 [7] proposed site response models that distinguish basins from other geomorphic provinces (valleys, mountain-hill regions), which were found to produce distinct amounts of long- and short-period amplification.

[1] Assistant Professor, USC, Civil and Environ. Eng., Los Angeles, CA, 90089. Email: ccnweke@usc.edu
[2] Professor, UCLA, Civil and Environ. Eng., Los Angeles, CA, 90095. Email: jstewart@seas.ucla.edu
[3] Post-Doctoral Scholar, UCLA, Civil and Environ. Eng., Los Angeles, CA, 90095. Email: wltcwpf@ucla.edu
[4] Professor, UCLA, Civil and Environ. Eng., Los Angeles, CA, 90095. Email: sjbrandenberg@ucla.edu

Nweke, C.C., Stewart, J.P., Wang, P., Brandenberg, S. J. Sedimentary Basin Site Response for Different Basin Types in Southern California. *Proceedings of the 12th National Conference in Earthquake Engineering*, Earthquake Engineering Research Institute, Salt Lake City, UT. 2022.

Moreover, because southern California contains a variety of sedimentary basins having different geologic origins, we investigate here whether site response conditioned on V_{S30} and isosurface depth varies between basins in a manner that can be linked to their geologic origin.

Basin Geology

Basins form in southern California in continental and oceanic settings. Fig. 1 shows eight major basin structures including the Los Angeles basin (LAB), the Ventura basin (VB), the San Fernando basin (SFB), the San Gabriel basin (SGB), the Chino basin (CB), the San Bernardino basin (SBB), the Coachella Valley basin (CVB), and the Imperial Valley basin (IVB). These basins can be further categorized into three general types. First, the three westernmost basins (LAB, VB, SFB), which were formerly connected, experienced intermittent subsidence and uplift that provided continental and oceanic sediment depositional environments [8]. These are referred to as coastal basins and they are deeper than other basins in the region. Second are the inland basins that have shallower depths and were formed as transform-graben induced valleys that were filled with sediments from erosion of the adjacent uplifted blocks [9,10]. This type of basin includes SGB, CB, SBB, and CVB. The third type is based on IVB and is identified as a step-over basin where a down-dropped graben is combined with volcanic and geothermal activity associated with local crustal spreading [11].

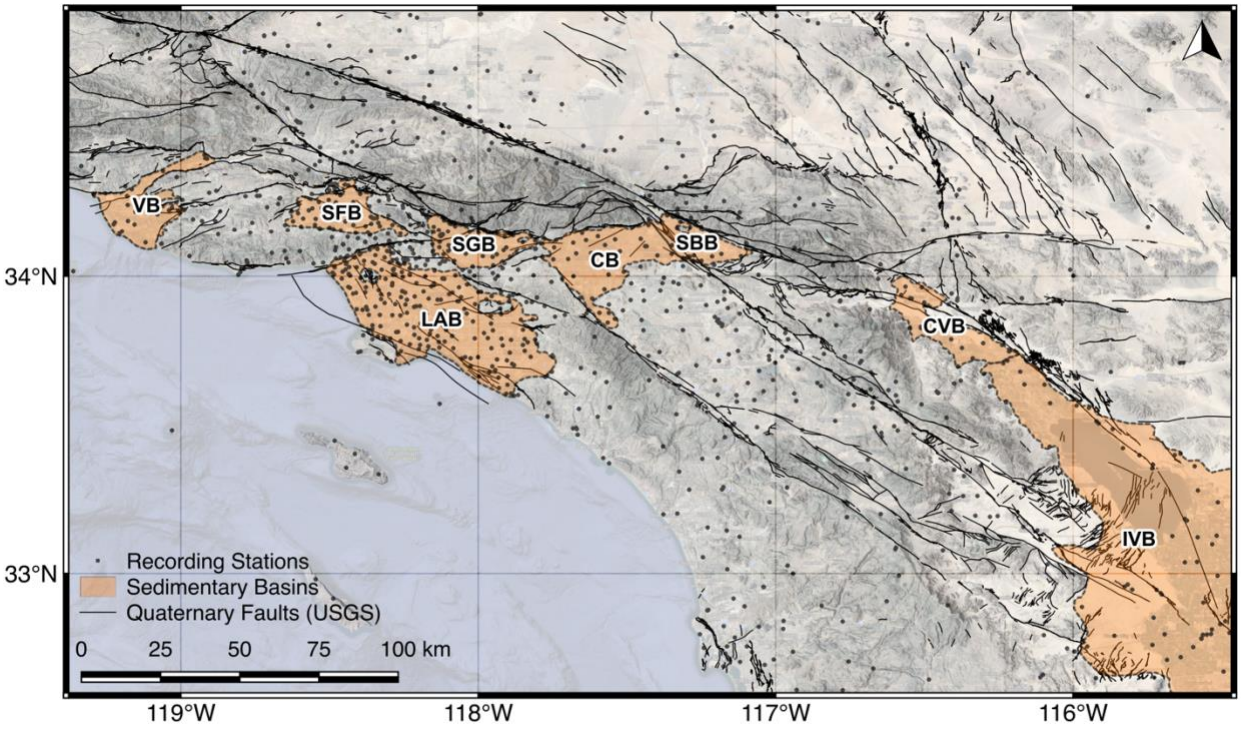

Figure 1. Map showing the locations of southern California basins, recording stations, and adjacent faults.

Database

A California-specific ground motion database [12, 13] has been developed to facilitate the analysis in this study. This database adopts the California-specific data from NGA-West2 [14] and supplements it with additional recordings and stations from events that have occurred since 2011 (termination of the NGA-West2 data aggregation). The total California database now has approximately 13,000 recordings at 1034 stations from 225 events. The site portion of the database has been updated with

respect to V_{S30} based on recent availability of measured data, and improved proxy combinations [15, 16]. The isosurface depths have also been updated to reflect the improvements in the southern California community velocity models, CVM-S4.26.M01 [17] and CVM-H v15.1 [18].

Residual Analysis

A residual, R_{ij}, is computed as the difference between the natural log of the recorded ground motion and a model prediction.

$$R_{ij} = ln(Y_{ij}) - \left[\mu_{ln,ij}\left(\mathbf{M}_i, F_i, (R_{jb})_{ij}, V_{S30}, z_{1.0}\right)\right] \quad (1)$$

where index i refers to an earthquake and index j refers to a recording station. The quantity Y_{ij} is a ground motion observation expressed as an intensity measure. The term $\mu_{ln,ij}$ is the mean prediction in natural log units of a ground motion model giving the parameters within the parentheses of Eq. 1. We employ the use of the Boore et al. 2014 GMM [19] where $\boldsymbol{M}$ is the moment magnitude, F is the style of faulting parameter, R_{jb} is the Joyner-Boore distance, and other parameters are as previously defined. From the residuals, using mixed-effects analysis [20], we remove random effects that have systematic differences associated with the events (event terms, η_E) to isolate those differences associated with the sites (site terms, η_S).

$$R_{ijk} = c_k + \eta_{E,ik} + \eta_{S,jk} + \varepsilon_{ijk} \quad (2)$$

where c_k is an overall model bias for ground motion model k and ε_{ij} is the remaining residual when the event and site terms have been removed. For a given intensity measure, the mixed-effects analysis provides estimates of c_k, η_E for all events, and η_S for all sites. The site terms used to assess the site response associated with basins are estimated based on residuals that do not incorporate basin effects ($z_{1.0}$ is omitted from the GMM arguments to keep its effects in the residuals) and categorized into respective basins following the outlines in Figure 1.

Mean Basin Site Response

Figure 2 shows the mean of the site terms for different basins in southern California plotted against oscillator period. The means across all basins combined exhibit a lack of bias for periods less than about 0.3 sec, but for longer periods the combined basin sites exhibit relative amplification (indicating under prediction) that peaks between 4-6 sec. The coastal basins (LAB, SFB) exhibit similar trends to the combined basin sites though LAB shows higher relative amplification at long periods. For short periods ($T < 0.8$) sec SFB exhibits higher relative amplification compared with the combined basin and LAB. The inland basins generally display relative de-amplification at long periods (CB, CVB, SBB) with SBB showing minimal bias. SGB is the exception with appreciable relative amplification at long periods. At short periods, there is no consistent behavior amongst the inland basins, with CVB and CB exhibiting relative amplification and the others (SBB, SGB) showing relative de-amplification. Similar to the coastal basins, the step-over basin (IVB) shows relative amplification at long periods but it also shows relative de-amplification at short periods. The mean of site terms for VB is not shown due to an insufficiently low number of sites (< 5 sites).

Discussion

The trends displayed in Figure 2 are generally aligned with expected site response physics. The deeper basins such as LAB, SFB, and IVB would have low resonant frequencies that manifest as significant long period site response and show as positive means. Whereas the shallow inland basins would resonate at higher frequencies and therefore exhibit null or negative means in site response at long

periods and positive means at short periods. The variations we observe from basin to basin, particularly between the inland basin types, may be explained by the three-dimensional nature of seismic wave interactions with their sedimentary structure. For example, Langenheim et al. 2011 [8] show that the SFB shape and orientation is complex with a deeper bowl-like Sylmar subbasin (approx. 8 km at its deepest) attached to the wedge-like Northridge valley basin (approx. 4 km) to look like a ladle or scoop from its cross-sectional view. This may be the reason for the positive relative amplification at long periods and some short periods, which is unlike other deep basins.

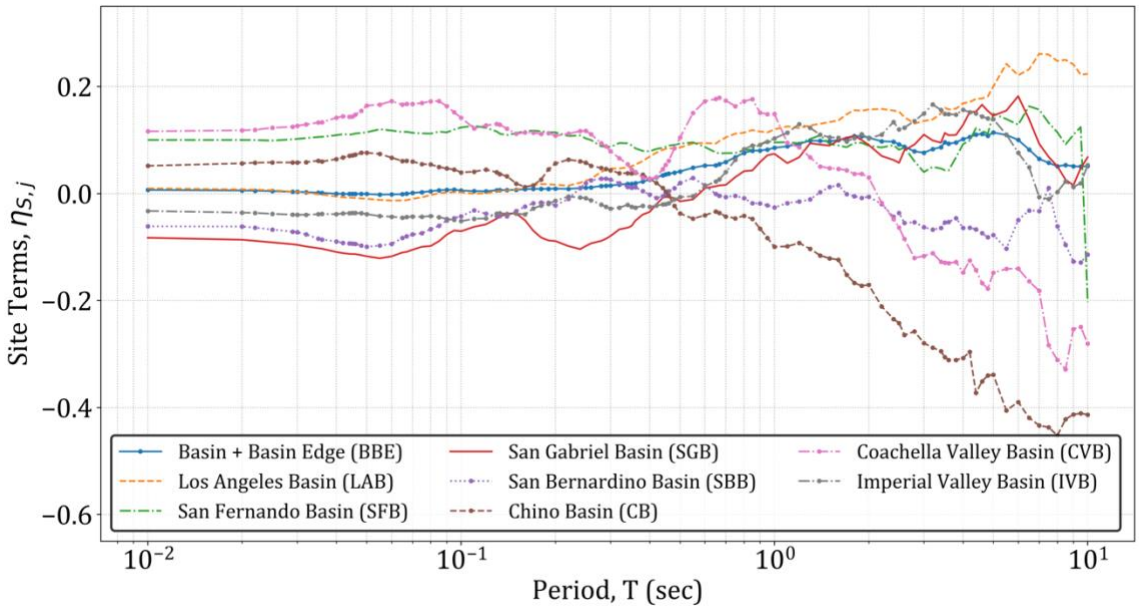

Figure 2. Mean of site terms for different sedimentary basins in southern California

Conclusion

The proposed individual basin categorization scheme was intended to differentiate the site responses between different basins in southern California and introducing them to the GMMs reveals features that are to some extent expected. For example, the deeper coastal basins with larger sedimentary deposits and structure have larger ground motions at long periods where their predominant periods resonate. Inland basins generally show relative amplification at shorter periods ($T < 0.2$ sec) where their predominant periods are expected to resonate. These observations suggest that the geologic history and evolution of sedimentary basins have a quantifiable impact on the site response beyond their effect on V_{S30} and isosurface depth. This is further investigated in an expanded study to discern the scaling features of the proposed basin types.

References

1. Einsele, G. (2000). Sedimentary basins: evolution, facies, and sediment budget. *Springer Science & Business Media*
2. Kingston, D. R., Dishroon, C. P., & Williams, P. A. (1983). Global basin classification system. *AAPG bulletin*, 67(12), 2175-2193.
3. Allen, P. A., and Allen, J. R., (2013). Basin Analysis: Principles and Application to Petroleum Play Assessment. *John Wiley & Sons*.
4. Arce, J. L., Layer, P. W., Macías, J. L., Morales-Casique, E., García-Palomo, A., Jiménez-Domínguez, F. J., Benowitz, J., & Vásquez-Serrano, A. (2019). Geology and stratigraphy of the Mexico basin (Mexico city), central trans-Mexican volcanic belt. *Journal of Maps*, 15(2), 320-332.

5. Paudyal, Y. R., Yatabe, R., Bhandary, N. P., & Dahal, R. K. (2013). Basement topography of the Kathmandu Basin using microtremor observation. *Journal of Asian Earth Sciences*, 62, 627-637.
6. Yerkes, R. F. (1965). Geology of the Los Angeles Basin, California:-an Introduction. US Government Printing Office.
7. Nweke, C.C., J.P. Stewart, P. Wang, S.J. Brandenberg, (2022). Site Response of Sedimentary Basins and other Geomorphic Provinces in Southern California, Accepted to *Earthquake Spectra*.
8. Langenheim, V. E., Wright, T. L., Okaya, D. A., Yeats, R. S., Fuis, G. S., Thygesen, K., & Thybo, H., (2011). Structure of the San Fernando Valley region, California: Implications for seismic hazard and tectonic history. *Geosphere*, 7, 528-572.
9. Graves, R. W. (2002). The seismic response of the San Bernardino basin region. AGUFM, 2002, S21A-0968.
10. Yeats, R.S., (2004). Tectonics of the San Gabriel Basin and surroundings, southern California. *GSA Bulletin*, 116(9-10), 1158-1182.
11. Lizarralde, D., Axen, G. J., Brown, H. E., Fletcher, J. M., González-Fernández, A., Harding, A. J., Holbrook, W.S., Kent, G.M., Paramo, P., Sutherland, F., & Umhoefer, P. J. (2007). Variation in styles of rifting in the Gulf of California. *Nature*, 448(7152), 466-469.
12. Buckreis, T.E., C.C. Nweke, P. Wang, P. Zimmaro, S.J. Brandenberg, S. Mazzoni, J.P. Stewart, 2021. Augmentation of NGA-West2 database for California with new data since 2011, Data report, doi: xx, in preparation.
13. Nweke CC, Stewart JP, Wang P, Brandenberg SJ and Buckreis TE (2022) Data files for ground motion studies pertaining to southern California basins and other geomorphic provinces. Available at: https://www.designsafe-ci.org/data/browser/public/designsafe.storage.published/ PRJ-3373v2, last accessed March 2022.
14. Ancheta, T.D., Darragh, R.B., Stewart, J.P., Seyhan, E., Silva, W.J., Chiou, B.S.-J., Wooddell, K.E., Graves, R.W., Kottke, A.R., Boore, D.M., Kishida, T., and Donahue, J.L., 2014. NGA-West2 database, *Earthquake Spectra*, 30, 989-1005.
15. Ahdi S.K., Mazzoni S., Kishida T., Wang P., Nweke C.C., Kuehn N.M., Contreras V., Rowshandel B., Stewart J.P., Bozorgnia Y., 2020. Engineering characteristics of ground motions recorded in the 2019 Ridgecrest earthquake sequence. *Bull. Seismol. Soc. Am.*, 110(4), 1474-1494.
16. Wang P., 2020. Predictability and repeatability of non-ergodic site response for diverse geological conditions. Ph.D. Dissertation, UCLA Civil & Environmental Engineering Department.
17. Lee E.J., Chen P., Jordan T.H., Maechling P.J., Denolle M., Beroza G.C., 2014. Full-3-D tomography for crustal structure in southern California based on the scattering-integral and the adjoint-wavefield methods, *J. Geophys. Res.*, 119, 6421–6451.
18. Shaw J.H., Plesch A., Tape C., Suess M.P., Jordan T.H., Ely G., Hauksson E., Tromp J., Tanimoto T., Graves R.W. et al., 2015. Unified structural representation of the southern California crust and uppermantle, *Earth Planet. Sci. Lett.*, 415, 1, doi: 10.1016/j.epsl.2015.01.016.
19. Boore D.M., Stewart J.P., Seyhan E., Atkinson G.M., 2014. NGA-West2 equations for predicting PGA, PGV, and 5% damped PSA for shallow crustal earthquakes. *Earthquake Spectra*, 30(3), 1057-1085.
20. Gelman, A., Carlin, J. B., Stern, H. S., Dunson, D. B., Vehtari, A., and Rubin, D. B., 2014. Bayesian Data Analysis, 3rd edition, CRC Press.